

# Modified Magnesium Hydroxide Nanoparticles Inhibit the Inflammatory Response to Biodegradable Poly(lactide-co-glycolide) Implants

Eugene Lih,<sup>†,^</sup> Chang Hun Kum,<sup>†,‡,^</sup> Wooram Park,<sup>§,^</sup> So Young Chun,<sup>+</sup> Youngjin Cho,<sup>⊥</sup> Yoon Ki Joung,<sup>†,#</sup> Kwang-Sook Park,<sup>†</sup> Young Joon Hong,<sup>∇</sup> Dong June Ahn,<sup>‡</sup> Byung-Soo Kim,<sup>○</sup> Tae Gyun Kwon,<sup>||</sup> Myung Ho Jeong,<sup>∇</sup> Jeffrey A. Hubbell,<sup>\*,&</sup> and Dong Keun Han<sup>\*,§</sup>

<sup>†</sup>Center for Biomaterials, Korea Institute of Science and Technology, Seoul 02792, Republic of Korea

<sup>‡</sup>Department of Chemical & Biological Engineering and KU-KIST Graduate School of Converging Science & Technology, Korea University, Seoul 02841, Republic of Korea

<sup>§</sup>Department of Biomedical Science, College of Life Sciences, CHA University, 335 Pangyo-ro, Bundang-gu, Seongnam, Gyeonggi 13488, Republic of Korea

<sup>+</sup>BioMedical Research Institute, Kyungpook National University Hospital, Daegu 41944, Republic of Korea

<sup>||</sup>Department of Urology, School of Medicine, Kyungpook National University, Daegu 37224, Republic of Korea

<sup>⊥</sup>Research Group of Food Storage & Distribution, Korea Food Research Institute, Wanju 55365, Republic of Korea

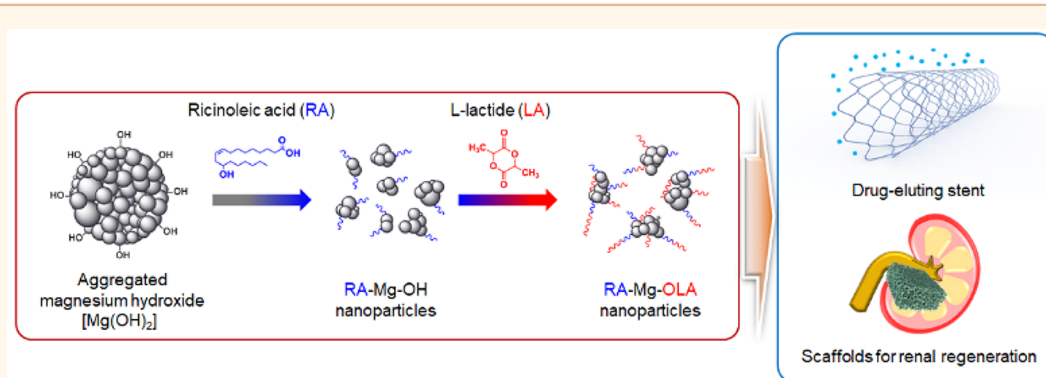
<sup>#</sup>Department of Biomedical Engineering, Korea University of Science and Technology, Daejeon 34113, Republic of Korea

<sup>∇</sup>The Heart Center of Chonnam National University Hospital, Gwangju 61469, Republic of Korea

<sup>○</sup>School of Chemical and Biological Engineering, Seoul National University, Seoul 08826, Republic of Korea

<sup>&</sup>Institute for Molecular Engineering, University of Chicago, Chicago, Illinois 60637, United States

## Supporting Information



**ABSTRACT:** Biodegradable polymers have been extensively used in biomedical applications, ranging from regenerative medicine to medical devices. However, the acidic byproducts resulting from degradation can generate vigorous inflammatory reactions, often leading to clinical failure. We present an approach to prevent acid-induced inflammatory responses associated with biodegradable polymers, here poly(lactide-co-glycolide), by using oligo(lactide)-grafted magnesium hydroxide (Mg(OH)<sub>2</sub>) nanoparticles, which neutralize the acidic environment. In particular, we demonstrated that incorporating the modified Mg(OH)<sub>2</sub> nanoparticles within degradable coatings on drug-eluting arterial stents efficiently attenuates the inflammatory response and in-stent intimal thickening by more than 97 and 60%, respectively, in the porcine coronary artery, compared with that of drug-eluting stent control. We also observed that decreased

*continued...*

Received: March 29, 2018

Accepted: May 29, 2018

Published: May 29, 2018

inflammation allows better reconstruction of mouse renal glomeruli in a kidney tissue regeneration model. Such modified  $\text{Mg}(\text{OH})_2$  nanoparticles may be useful to extend the applicability and improve clinical success of biodegradable devices used in various biomedical fields.

**KEYWORDS:** biodegradable polymers, inflammation, magnesium hydroxide, neutralization, biomedical applications

Biodegradable synthetic polymers have attracted considerable attention in the field of biomedical research because of some intrinsic properties such as batch uniformity, predictable degradation rates, ease of chemical modification, and optimal control over mechanical properties. Moreover, hydrolytically degradable polyesters derived from lactic acid, glycolic acid, and other  $\alpha$ -hydroxyl acids such as poly(lactic-co-glycolic acid) (PLGA) have been widely used as effective materials in tissue engineering, regenerative medicine, drug delivery systems, surgical implants, and medical devices.<sup>1–4</sup> Nevertheless, inherent shortcomings remain associated with PLGA including induced inflammation due to the acidic degradation products.<sup>5,6</sup> Although the acidic byproducts (*i.e.*, lactic acid and glycolic acid) of PLGA are finally absorbed by the Krebs cycle,<sup>7</sup> chronic inflammation can result from their local presence, limiting clinical success with these important polymers in several applications, including vascular interventions and tissue engineering.<sup>8</sup> A recent example of a clinical disappointment can be seen in a 3 year, >300 patient studies of an everolimus-releasing poly(lactide)-based absorbable vascular scaffold used in coronary artery dilation, which did not perform as well in late lumen loss as a biostable polymer-coated metal stent releasing the same drug;<sup>9</sup> this unfavorable result might be derived from tissue reactions associated with degradation products.

To address these limitations, a large body of literature has investigated multiple mixing strategies for preventing cell death and inflammation following implantation of PLGA.<sup>10–12</sup> Most notably, Isakawa *et al.* reduced PLGA-induced inflammation in fibroblast cells by blending 2-methacryloyloxyethyl phosphorylcholine polymer, a cell membrane mimic, with PLGA.<sup>10</sup> Yoon *et al.* reported increased cell viability and decreased expression of inflammatory cytokines after enriching PLGA with demineralized bone particles, which induce bone growth.<sup>11</sup> Li *et al.* reported decreased inflammatory reactions due to pH buffering effects of hydroxyapatite incorporated in degrading PLGA scaffolds.<sup>12</sup> Even though these attempts reduced inflammatory response by promoting cell growth, absolutely nothing was resolved in the essential cause of acid-induced inflammation resulting from PLGA degradation.

In a previous study, we showed that the byproducts of degraded PLLA were effectively neutralized by magnesium hydroxide ( $\text{Mg}(\text{OH})_2$ ) particles despite the poor dispersion of aggregated  $\text{Mg}(\text{OH})_2$  in PLLA matrices.<sup>13</sup> When compared to other biodegradable materials such as poly-L-lactide (PLLA), PLGA shows the faster onset of inflammatory responses triggered by its rapid degradation.<sup>14</sup> PLLA degradation is known to occur over 1–2 years *in vivo* owing to its high crystallinity and resistance to hydrolysis.<sup>15–17</sup> By contrast, the degradation of 100 kDa PLGA with a lactide-to-glycolide ratio of 1:1 occurs within 8 weeks *in vivo*.<sup>18–20</sup> Also, PLGA biodegradation rates increase at lower molecular weights and depend on the molar ratio of lactide and glycolide. The penetration of water rapidly occurs through the amorphous regions and contributes to the degradation of PLGA by hydrolysis of its ester linkages. The ester hydrolysis inevitably produces acidic byproducts which tend to accumulate in the center of polymer matrix and induce autocatalysis leading to a further increase in the rate of hydrolysis and resulting in bulk or heterogeneous erosion of polymer matrix.<sup>21,22</sup>

At this rate, the aggregated  $\text{Mg}(\text{OH})_2$  particles in PLGA matrix will not sufficiently neutralize the acidic degradation products. The aggregated  $\text{Mg}(\text{OH})_2$  may have accelerated degradation reaction of PLGA by attacking the backbone of contacting polymer rather than dispersedly and uniformly dissociating into  $\text{Mg}^{2+}$  and  $\text{OH}^-$  ions and neutralizing the acidic byproducts. Although the reactions to foreign bodies are minimized by rapid degradation and elimination of PLGA, tissue damage still occurs due to the formation of acidic materials over a short period.<sup>23,24</sup>

In this study, we report the suppression of PLGA byproduct-triggered cell death and inflammation by using a neutralization system based on the incorporation of  $\text{Mg}(\text{OH})_2$  nanoparticles. Achieving this feature required us to overcome  $\text{Mg}(\text{OH})_2$  aggregation in nonpolar organic solvents.<sup>25</sup> This was done by using hydrophobic nanosized  $\text{Mg}(\text{OH})_2$  particles. To modulate the homogeneous state of  $\text{Mg}(\text{OH})_2$  in organic solvents, we changed the polarity of  $\text{Mg}(\text{OH})_2$  from a hydrophilic to a hydrophobic state by grafting lipid ligands onto the surfaces of the particles.<sup>25–27</sup> We chose ricinoleic acid (RA) as the lipid ligand. RA has a hydroxyl group that can act as an initiator for polymerization of L-lactide (L-LA) and is known to have an anti-inflammatory effect.<sup>28</sup> Finally, oligolactide-grafted  $\text{Mg}(\text{OH})_2$  (RA-Mg-OLA) was prepared by ring-opening polymerization (ROP) of L-lactide (L-LA), leading to prevention of aggregation of  $\text{Mg}(\text{OH})_2$  nanoparticles (Figure 1). The surface modified

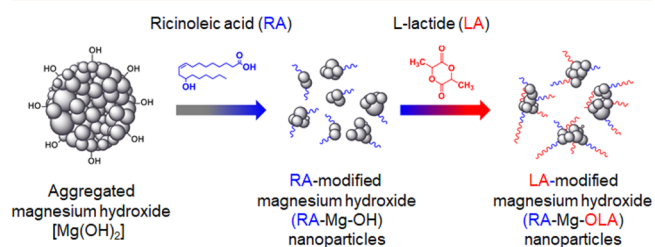


**Figure 1.** Preparation of RA-Mg-OLA nanoparticles to neutralize PLGA matrices. RA-Mg-OH was prepared by modifying the surface of Mg-OH particles with ricinoleic acid (RA), and RA-Mg-OLA was prepared by ring-opening polymerization (ROP) of L-lactide (5–20 wt %) from the RA hydroxyl group on RA-Mg-OH.

$\text{Mg}(\text{OH})_2$  nanoparticles uniformly dispersed in PLGA matrix could improve the mechanical properties of PLGA-based medical devices and neutralize the acidic degradation products of PLGA to inhibit the inflammatory response.

## RESULTS AND DISCUSSION

To synthesize surface-modified  $\text{Mg}(\text{OH})_2$  nanoparticles with OLA, a two-step process was performed as described above. First, RA was bonded to the surface of the  $\text{Mg}(\text{OH})_2$  nanoparticles at different ratios (Figure S1 and Table S1). Next, the RA-Mg-OLA was synthesized using the hydroxyl group of RA on the surface of the  $\text{Mg}(\text{OH})_2$  as an initiator for OLA. The RA-Mg-OLA were synthesized by ROP of L-LA (Figure 1): a series of RA-Mg-OLAs obtained from RA-Mg-OH and L-LA were produced according to feed ratios of Mg-OHs (Table S1). The obtained  $\text{Mg}(\text{OH})_2$  nanoparticle size was  $209 \pm 101$  nm when not modified.

A significant reduction to  $43 \pm 13$  nm was obtained when the modification with RA was introduced (Figure S1 and S2). We also observed that RA15-Mg-OLA nanoparticle sizes increased as a function of OLA content (0–20 wt %; Figure 2a).

PLGA (MW, 40 kDa) composites of PLGA/Mg(OH)<sub>2</sub>, PLGA/RA15-Mg-OH 15 wt %, PLGA/RA15-Mg-OLA5 5 wt %, and PLGA/RA-Mg-OLA 15 wt % were prepared, and the morphology, elemental distributions, neutralization effect, and mechanical properties were investigated (the percentage is the weight percent of the Mg(OH)<sub>2</sub> nanoparticles or their derivatives relative to the total weight of PLGA composites). Morphological analyses of PLGA/RA15-Mg-OLA5 (both 5 and 15 wt %) indicated smooth surfaces and highly uniform Mg element distributions compared with those of the PLGA control, PLGA/Mg(OH)<sub>2</sub>, and PLGA/RA15-Mg-OH (Figure S3). These observations indicate a good hydrophobic interaction between RA15-Mg-OLA5 and the surrounding PLGA matrix, whereas Mg(OH)<sub>2</sub> alone and RA15-Mg-OH formed aggregates due to hydrogen bonds between Mg(OH)<sub>2</sub> nanoparticles. Furthermore, previously reported differences in surface roughness between the polymer containing pure Mg(OH)<sub>2</sub> and modified Mg(OH)<sub>2</sub><sup>29</sup> were confirmed by the present contact angles measurements and scanning electron microscope (SEM) images (Figure S3). Based on these results, we selected RA15-Mg-OLA5 with the best dispersion stability with sub 100 nm size and performed the following experiments.

Next, the mechanical properties of PLGA/Mg(OH)<sub>2</sub>, PLGA/RA15-Mg-OH, and PLGA/RA15-Mg-OLA5 composites with various particle contents (wt %) were investigated using a universal testing machine (UTM) (Figure 2b and Figure S5). We found that the tensile strength of PLGA films containing RA15-Mg-OH or RA15-Mg-OLA5 increased from 4 to 8 and 12 MPa respectively, with increasing concentrations to 20 wt %. In contrast, the tensile strength of PLGA/Mg(OH)<sub>2</sub> containing films decreased from 4 to 2 MPa under the same conditions (Figure 2b). Subsequently, the interfacial interaction parameter (*B* value) was calculated for evaluating interaction forces between PLGA films and Mg(OH)<sub>2</sub> nanoparticles.<sup>30</sup> *B* values at any relative yield stress showed the positive contributions of RA15-Mg-OH and RA15-Mg-OLA5 to the mechanical properties of the PLGA matrix. Accordingly, *B* values for PLGA/Mg(OH)<sub>2</sub>, PLGA/RA15-Mg-OH, and PLGA/RA15-Mg-OLA5 composites were 0.276, 6.286, and 9.274, respectively (Figure 2c).

In a second step, we aimed at quantifying the impact of embedding modified Mg(OH)<sub>2</sub> nanoparticles on the acidification of the cellular microenvironment. Figure 2d showed that PLGA, PLGA/Mg(OH)<sub>2</sub> (15 wt %), PLGA/RA-Mg-OH (15 wt %), and PLGA/RA15-Mg-OLA5 (5 and 15 wt %) composite degradation (37 °C and 100 rpm for 120 days) had different impact on the acidification of the milieu. Native PLGA induced a rapid drop of pH to around pH 4 at day 7 and maintained pH values below 3 for a while after that, whereas the pH of PLGA/Mg(OH)<sub>2</sub> and PLGA/RA15-Mg-OH composites decreased to 5.6 and 6.3 respectively in 28 days, the pH increasing gradually afterward. These observations suggest the accelerated formation of an acidic environment following the abrupt degradation of the PLGA film from the onset of the experiment to day 28 stemmed in an insufficient neutralization of PLGA byproducts by the amounts of Mg(OH)<sub>2</sub> and RA15-Mg-OH present in the studied composites. In contrast, the pH of PLGA/RA15-Mg-OLA5 (15 wt %) was maintained at close to neutral pH 7.1 for 28 days by equilibrating pH levels between acidic degradation products and sustained release of magnesium ions (Figure 2d and Figure S4e).

The inherent acidity of PLGA degradation could harmfully affect cell activity and viability because of a highly acidic condition below pH 3, which has been shown to cause unfolding of proteins and accelerated peptide bond hydrolysis in sustained-release protein formulations.<sup>31</sup> When PLGA composites (PLGA/RA15-Mg-OLA5, 0 to 20 wt %) were introduced into cultures of human umbilical vein endothelial cells (HUVECs), we found that the number of live cells increased with increases in RA15-Mg-OLA5 contents from 0 to 20 wt %, and cell viability approached 90% in the presence of 10 wt % RA15-Mg-OLA5 (Figure 2e), reflecting a good neutralization of acidic byproducts (Figure 2d and Figure S4b). Moreover, we performed ELISA analysis on treated HUVECs (Figure 2f) to quantify the interleukin response upon exposure to the PLGA composites. We found that high expression of IL-6, an important inflammatory factor, was triggered by the presence of 5 wt % of RA15-Mg-OLA5 in the PLGA composite. On the other hand, IL-6 significantly dropped to control levels when 10–20 wt % of RA15-Mg-OLA5 composite was used. Similarly, when TNF- $\alpha$  expression was quantified in treated U937 cells, a monocyte cell line, similar profiles were obtained when compared to IL-6 expression in HUVECs (Figure S6). To further assess the anti-inflammatory effects of RA15-Mg-OLA5, the mechanism of HUVECs death was scrutinized by separating between necrosis and apoptosis processes. Flow cytometry (Figure 2g) and fluorescent microscopy (Figure 2h) using a commercial annexin V-FITC/propidium iodide (PI) kit showed that the degradation products of PLGA/RA15-Mg-OLA5 decreased approximately 80% of double positive (annexin V and PI) cells compared with PLGA treated controls. It also showed lower rates of the early apoptotic cells (annexin V<sup>+</sup>/PI<sup>-</sup> cells). This demonstrates that RA15-Mg-OLA5 addition ameliorates necrotic cell death following PLGA degradation.

The applicability of surface-modified Mg(OH)<sub>2</sub> nanoparticles in the biodegradable polyester matrix was investigated further in multiple *in vivo* studies including intracoronary stenting in a porcine model for the neointimal formation and mouse partial nephrectomy model for reconstruction of renal glomerular tissue. To assess the feasibility of PLGA and modified Mg(OH)<sub>2</sub> composites as biodegradable coating materials for drug-eluting stent (DES) in the coronary artery, sirolimus-loaded PLGA-coated (DES control) and sirolimus-loaded PLGA/RA15-Mg-OLA5-coated (DES/RA-Mg-OLA; where the RA15-Mg-OLA5 was incorporated at 20 wt %) cobalt–chromium stents were implanted in the major branches of the coronary arteries of pigs. Since unmodified Mg(OH)<sub>2</sub> particles cannot be dispersed in volatile solvents, it is difficult to apply the bare Mg(OH)<sub>2</sub> to the ultrasonic spray-coating process. Thus, the PLGA/Mg(OH)<sub>2</sub> group was excluded from the experimental groups. At 28 days follow-up, hematoxylin and eosin (H&E) and Carstairs' fibrin staining revealed that the number of inflammatory cells and fibrin infiltrates surrounding the struts of the DES control sections was greater than that of the surrounding DES/RA-Mg-OLA (Figure 3a–d). Moreover, the internal elastic lamina (IEL) and lumen areas increased, whereas injury scores, neointimal areas, stenosis areas, fibrin scores, and inflammation scores were significantly reduced in DES/RA-Mg-OLA when compared to those of DES control (Table S2 and Figure 3e–k). Percent area of stenosis in microcomputed tomography analysis showed a significant difference (20.5% in DES control vs 14.1% in DES/RA-Mg-OLA,  $p < 0.01$ ; Figure 3i and m), *i.e.*, that DES with RA-Mg-OLA was more effective at preventing in-stent restenosis (ISR) than the DES control. Accordingly, injury and inflammation

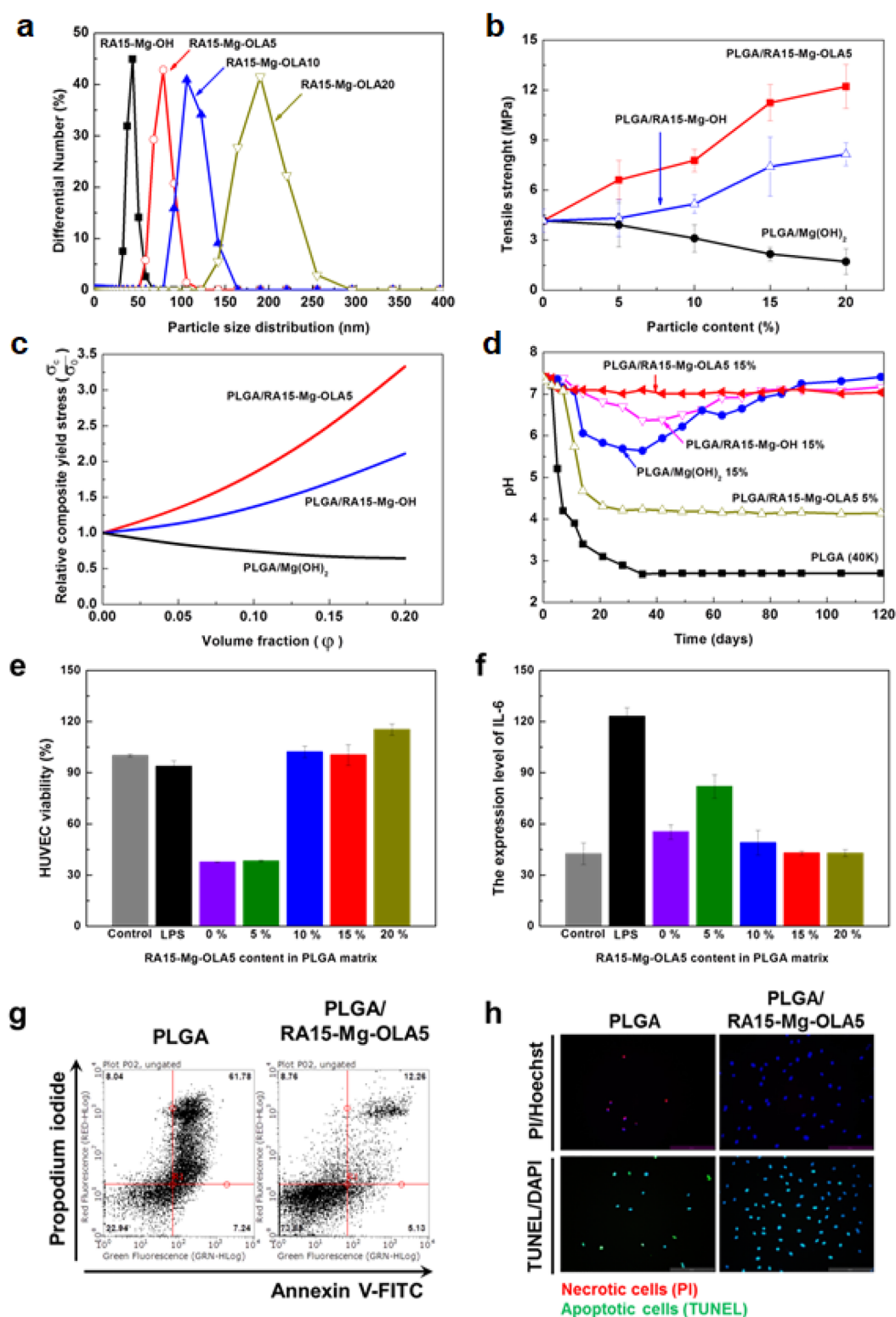


**Figure 2.** Nanosized RA-Mg-OLA particles and the PLGA/RA-Mg-OLA composite. (a) Particle-size distributions of surface-modified RA-Mg-OLAs in toluene. (b, c) Tensile strengths and relative yield stress *versus* volume fractions of PLGA/Mg(OH)<sub>2</sub>, PLGA/RA15-Mg-OH, and PLGA/RA15-Mg-OLA5 composites were determined using a universal testing machine (UTM). (d) pH changes of PLGA control, PLGA/Mg(OH)<sub>2</sub>, 15 wt %, PLGA/RA15-Mg-OH 15 wt %, PLGA/RA15-Mg-OLA5 5 wt %, and PLGA/RA15-Mg-OLA5 15 wt % were measured in PBS for 120 days. (e, f) Cell viability and IL-6 expression in human umbilical vein endothelial cells (HUVECs) cultured on PLGA and PLGA/RA-Mg-OLA films with varying concentrations of modified Mg(OH)<sub>2</sub> particles were analyzed using CCK-8 and ELISA kits, respectively. (g, h) Apoptosis and necrosis of HUVECs were determined using flow cytometry and fluorescent microscopy with a commercial Annexin V-FITC/propidium iodide (PI) kit.

induced the formation of neointima due to acidic degradation byproducts of the PLGA coating. However, DES with the

modified Mg(OH)<sub>2</sub> nanoparticles alleviated the inflammatory responses by more than 97% and led to a 60% reduction in

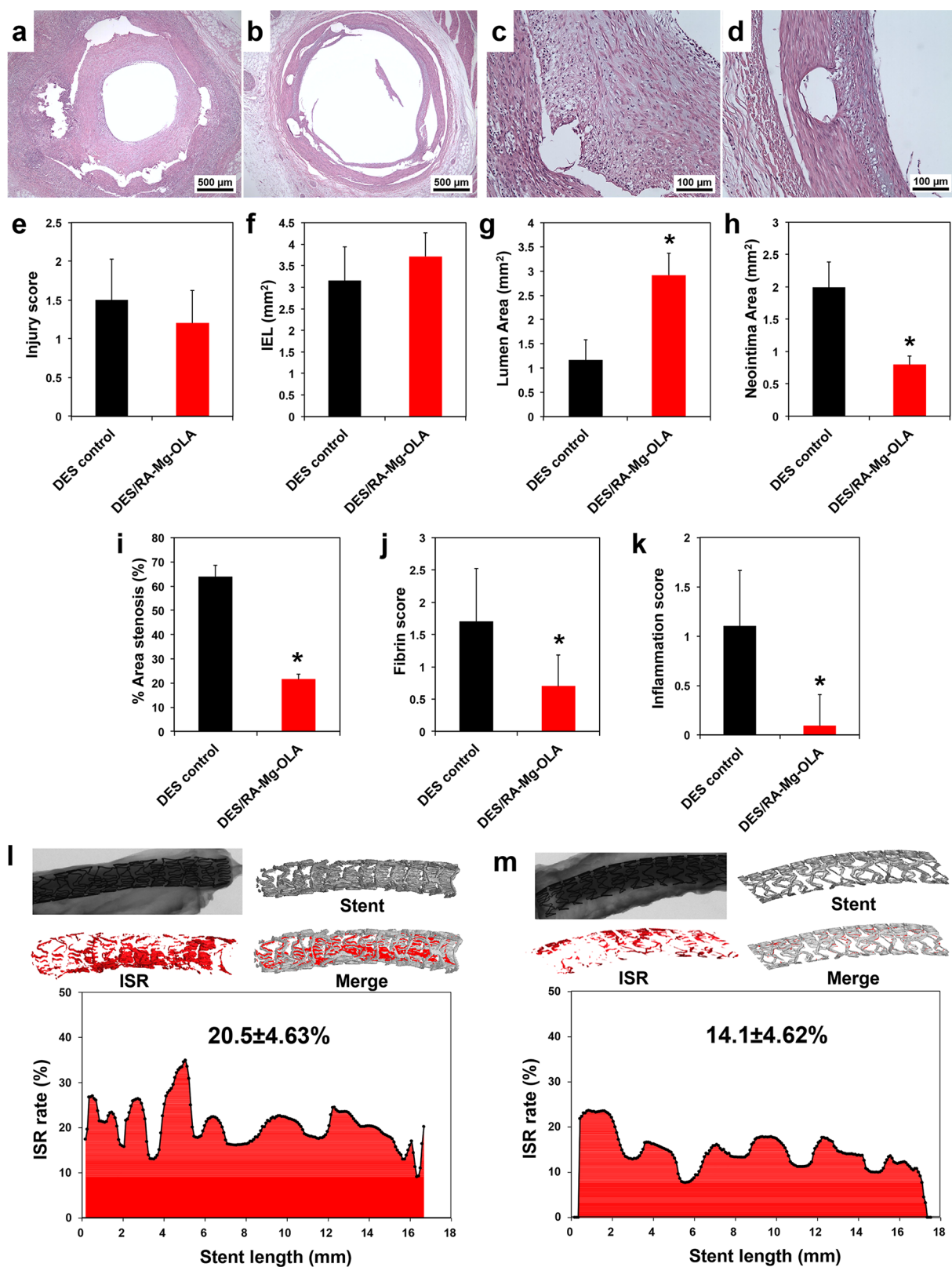


**Figure 3.** *In vivo* coronary implants of sirolimus-loaded PLGA coating stents (DES control) and DES containing modified magnesium hydroxide (DES/RA-Mg-OLA). Representative H&E staining images at 4 weeks after stenting of implanted (a) DES control and (b) DES/RA-Mg-OLA specimen (magnification,  $\times 40$ ). Carstairs' fibrin staining of fibrin infiltration in low-power fields (magnification,  $\times 40$ ) of implanted (c) DES control and (d) DES/RA-Mg-OLA specimens. Histomorphometric scores: (e) injury score; (f) internal elastic lamina (IEL) area; (g) lumen area; (h) neointimal area; (i) % area stenosis; (j) fibrin score; and (k) inflammation scores in DES control and DES/RA-Mg-OLA groups;  $N = 10$  per group; ANOVA,  $*p < 0.001$  versus DES control group. Microcomputed tomography analyses of in-stent restenosis in (l) DES control and (m) DES/RA-Mg-OLA groups.

neointima formation. These results suggest that PLGA containing the modified  $\text{Mg}(\text{OH})_2$  nanoparticles could be applied as a coating material for biomedical devices, such as coronary artery stents.

To evaluate inflammation in the context of renal regeneration, PLGA, PLGA/ $\text{Mg}(\text{OH})_2$ , and PLGA/RA15-Mg-OLA5 scaffolds were implanted into mouse kidneys. Visual inspection showed that PLGA, PLGA/ $\text{Mg}(\text{OH})_2$ , and PLGA/RA15-Mg-OLA5 scaffolds were almost fully degraded after about 4 weeks (Figure S8). Histological and immunohistochemical (IHC) analyses showed that PLGA/RA15-Mg-OLA5 (15 wt %) scaffolds led to greater cell densities and glomerular-like structures than PLGA control and PLGA/ $\text{Mg}(\text{OH})_2$  at 1 week postimplantation. Similarly, the PLGA/RA15-Mg-OLA5 group showed higher numbers and increased sizes of glomeruli compared to the other groups at 4 weeks postimplantation, and distal, and proximal convoluted tubules were observed only in the PLGA/RA15-Mg-OLA5 group (Figure 4a,e). In quantitative microanatomy assessment of regenerated glomeruli at 4 weeks postimplantation (Figure 4e,f), we found that the number of glomeruli in scaffolds containing  $\text{Mg}(\text{OH})_2$  nanoparticles increased more than 10-fold when compared to the native PLGA control. The PLGA/RA15-Mg-OLA5 scaffold showed an even better 15-fold increase (Figure 4f). IHC analyses showed that inflammatory proteins were significantly less secreted in PLGA/RA15-Mg-OLA5 (Figure 4b and Figures S9–S11). These observations were also further confirmed in quantitative PCR analyses (Figure 4c,d and Figures S12–S14). In addition, the expression of mesenchymal stem cell-related markers increased at 2 weeks postimplantation, and the differentiation markers for renal cell lineages gradually increased (Figure S15). Taken together, these data indicate that the use of PLGA/RA15-Mg-OLA5 scaffolds increases the expression of mesenchymal stem cell and renal differentiation markers compared with other scaffolds. The suppression of inflammatory reaction on PLGA/RA15-Mg-OLA5 scaffolds reflects the neutralizing action of the modified  $\text{Mg}(\text{OH})_2$  nanoparticles and the secretion of anti-inflammatory factors by bone marrow stem cells.<sup>32</sup>

## CONCLUSION

In the present study, we addressed one of the most long-standing problems associated with the use of PLGA biodegradable scaffolds, namely acid-induced inflammation triggered by the byproducts of the polymer degradation. Incorporation of native  $\text{Mg}(\text{OH})_2$  into drug delivery carriers has been used to protect encapsulated protein payload from degradation.<sup>31</sup> In our applications for improvement of the biocompatibility of PLGA implants, we needed to develop hydrophobically modified nanoparticles rather than native  $\text{Mg}(\text{OH})_2$  to achieve adequate dispersal to enable adequately high loading for neutralization, which was also associated with increases in mechanical properties with the modified  $\text{Mg}(\text{OH})_2$  rather than decreases with the native  $\text{Mg}(\text{OH})_2$ . Thus, incorporation of modified nanoparticles comprising the  $\text{Mg}(\text{OH})_2$  surface functionalized with oligomers of lactide significantly reduced the *in vivo* inflammatory response without altering the degradability rates but improving the mechanical properties of PLGA. We showed across two distinct biomedical applications that our strategy could help with ameliorating the shortcomings associated with PLGA and perhaps improving the ease the transition to the clinic of a new generation of biodegradable polyester implants.

## MATERIALS AND METHODS

**Materials.** Magnesium nitrate ( $\text{Mg}(\text{NO}_3)_2$ ), stannous octoate, sodium hydroxide (NaOH), and ricinoleic acid (RA) were purchased

from Sigma-Aldrich (St. Louis, MO). L-Lactide (L-LA) was purchased from Boehringer Ingelheim (Ingelheim, Germany) and used after purification process through recrystallization. PLGA (LA/GA 50:50, MW 40000) was purchased from Evonik Industries (Essen, Germany). The stannous octoate was dissolved in distilled toluene at a concentration of 1 wt %.

U-937 cells (monocytes), HUVECs, and endothelial growth medium-2 (EGM-2) were obtained from Korean Cell Line Bank (Seoul, Korea) and Lonza (Switzerland). Enzyme-linked immunosorbent assay (ELISA) kits for IL-6 and TNF- $\alpha$  were purchased from R&D Systems Inc. (Minneapolis, MN). Roswell Park Memorial Institute medium (RPMI 164), monoclonal antibodies against  $\beta$ -actin, and polyclonal horseradish peroxidase-conjugated anti-IgG antibodies were purchased from Invitrogen (Tokyo, Japan), Santa Cruz Biotechnology (Santa Cruz, CA), and Abcam (Cambridge, UK) respectively.

**Modification of  $\text{Mg}(\text{OH})_2$  Nanoparticles.** Magnesium nitrate and sodium hydroxide were dissolved in distilled water at concentrations of 130 and 36 mg/mL, respectively, and stirred for 30 min at room temperature. The magnesium nitrate solution was dropped into the sodium hydroxide solution with 40 drops per min using a dropping funnel. As a result, 6.8 g of  $\text{Mg}(\text{OH})_2$  nanoparticles was obtained. Next, RA-modified  $\text{Mg}(\text{OH})_2$  nanoparticles (*i.e.*, RA15-Mg-OH) were synthesized by homogenizing mixtures of the as-synthesized  $\text{Mg}(\text{OH})_2$  nanoparticles (10 g) and RA (9 g). The mixture of  $\text{Mg}(\text{OH})_2$  nanoparticles and RA was dissolved in 250 mL of distilled water, homogenized at 15000 rpm for 3 min, and refluxed at 80 °C for 8 h. Subsequently, the phase separation occurred between RA-modified  $\text{Mg}(\text{OH})_2$  nanoparticles and water due to the hydrophobic properties of RA. The prepared RA-modified magnesium hydroxide (RA-Mg-OH) nanoparticles were dehydrated in a vacuum oven at 60 °C for 24 h after filtering, resulting in 11.61 g of RA-Mg-OH. The series of RA-Mg-OH preparations were coded according to feed ratios of  $\text{Mg}(\text{OH})_2$  and RA as follows: RA5-Mg-OH, RA10-Mg-OH, and RA15-Mg-OH (Table S1).

To carry out ROP from the surface of  $\text{Mg}(\text{OH})_2$  nanoparticles, the synthesized RA15-Mg-OH (10 g) nanoparticles and L-LA (5 g) were dissolved in 100 mL of toluene together with stannous octoate (8.34 mg) as a catalyst and reacted in a nitrogen atmosphere at 100 °C for 24 h. The final product was dissolved in chloroform and purified by centrifugation at 15000 rpm for 15 min to remove free PLLA and unreacted materials. After two repetitions of the purification process, the final material was vacuum dried at 60 °C for 24 h. The synthesis yield was 62.7–83.9%. The series of RA-Mg-OLAs from RA15-Mg-OH and L-LA were named according to feed ratios of  $\text{Mg}(\text{OH})_2$  and L-LA as follows: RA15-Mg-OLA5, RA15-Mg-OLA10, and RA15-Mg-OLA20 (Table S1).

**Fabrication of PLGA Composite Films and Scaffolds.** For further characterization, PLGA and RA-Mg-OLA nanoparticles were fabricated as solvent-cast films. PLGA (2 g) and RA15-Mg-OLA5 (0.3 g) were dissolved in 100 mL of chloroform at room temperature. The mixture of the polymer and nanoparticles was placed in a Teflon dish, and the solution was evaporated at room temperature for 24 h. The formed film was vacuum-dried at room temperature for 24 h. The film was removed from the Teflon dish using liquid nitrogen. The film thickness was measured using a micrometer and confirmed to be about 2 mm.

The porous 3D scaffold was fabricated through the ice particle method. First, 200–300  $\mu\text{m}$  sized ice particles were prepared by spraying cold distilled water into liquid nitrogen. PLGA (1 g) and the prepared ice particles (3 g) were dissolved in 4 mL of methylene chloride. The mixture was poured into a silicone mold contained in liquid nitrogen for freezing. The frozen mixture was lyophilized for 2 days to form porous scaffolds.

**Preparation of Drug-Eluting Stent.** Sirolimus-eluting stents with PLGA only or RA15-Mg-OLA5/PLGA were prepared by an ultrasonic nanocoating method. Briefly, PLGA (0.5% (w/w)) was dissolved in a cosolvent of dioxane and dichloromethane (1:1), and SRL or RA15-Mg-OLA5/SRL were then added to polymer solutions. Cobalt–chrome stents were spray coated with the polymer/nanoparticles solutions (10 mL) at a flow rate of 0.5 mL/min. The humidity in the coating chamber was maintained at 15% (NNC-30K-2 mA Portable type, Nano

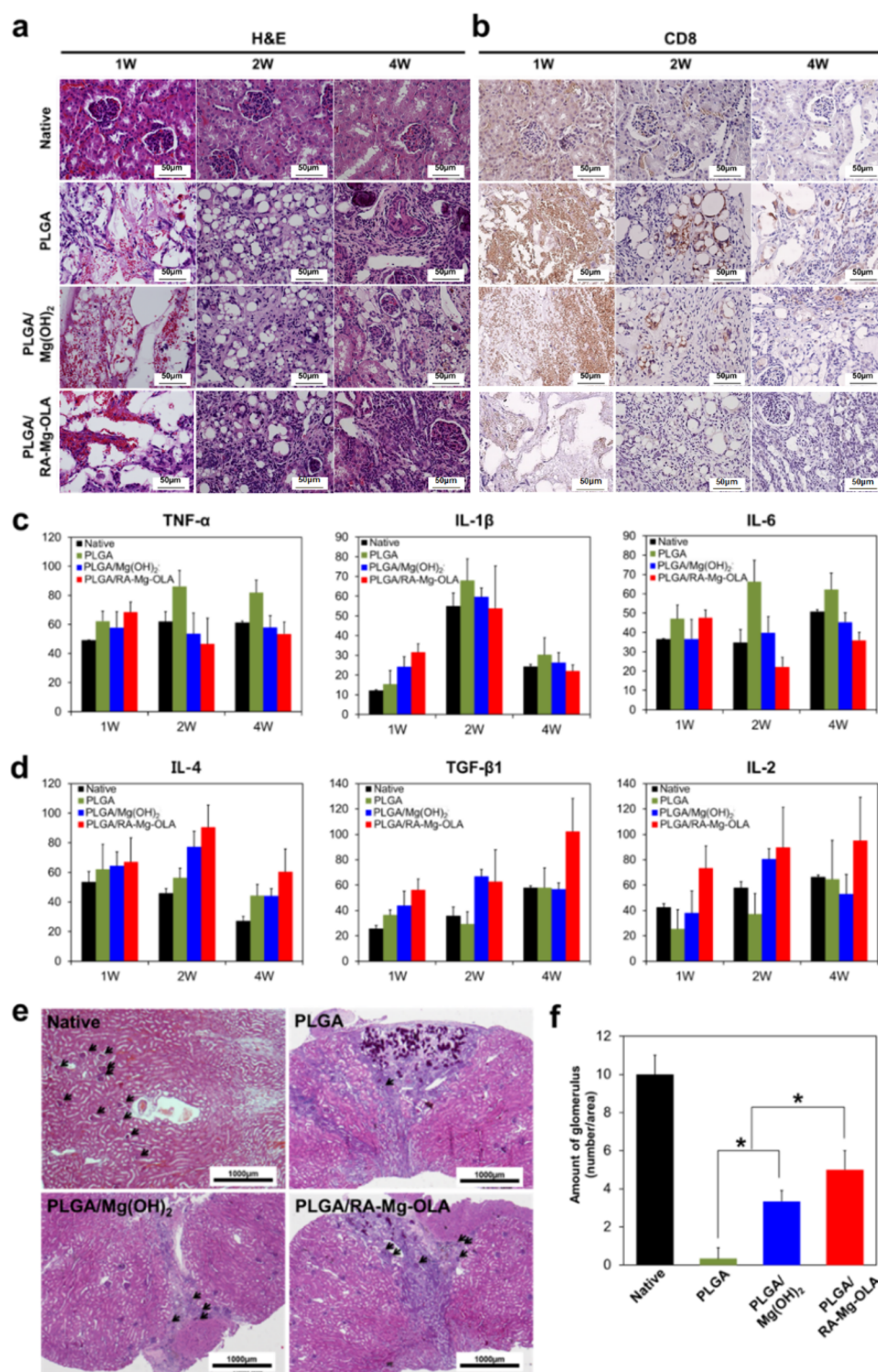


**Figure 4.** Reconstruction of injured kidney cortices with PLGA, PLGA/Mg(OH)<sub>2</sub>, and PLGA/RA-Mg-OLA scaffolds after partial nephrectomy. (a) Representative H&E staining of implanted scaffolds at 1, 2, and 4 weeks (scale bar, 50 μm). (b) Immunohistochemical (IHC) staining of CD8 in tissue sections of PLGA, PLGA/Mg(OH)<sub>2</sub>, and PLGA/RA-Mg-OLA scaffolds implanted in mice (scale bar, 50 μm). (c, d) Real-time PCR analysis of gene expression of (c) pro-inflammatory (TNF-α, IL-1β, and IL-6) and (d) anti-inflammatory markers (IL-4, TGF-β1, and IL-2). (e) Representative H&E staining of implanted scaffolds for assessment of regenerated glomeruli at 4 weeks postimplantation (black arrow indicates the regenerated glomeruli, scale bar, 1000 μm). (f) Quantitative analysis of regenerated glomeruli at 4 weeks postimplantation.

NC, Korea). Finally, the coated stents were vacuum-dried for 3 days to remove residual solvents.

**Characterization of Materials.** The RA-Mg-OLAs were structurally analyzed using Fourier transform infrared (FT-IR) spectroscopy (Spectrum 100, PerkinElmer, USA) with potassium bromide pellets. The molecular weight of the polymer was analyzed by gel permeation

chromatography (GPC; 414 GPC system, Waters, USA). The average molecular weight ( $M_w$ ) of PLGA used in this study was 41000 Da. To thermally analyze the synthesized compounds, thermogravimetric analysis (TGA) thermograms were measured in a nitrogen atmosphere at a heating rate 10 °C/min and a temperature range of 100–800 °C. The particle size distribution of RA-Mg-OLAs was measured by dynamic

light scattering (DLS; Malvern ZetaSizer Nano ZS, Malvern, UK). The morphology of nanoparticles dispersed in toluene was observed using TEM (Tecnai G2 F20 Cryo, FEI, USA). The surface morphology and atomic distribution of nanocomposites were observed using SEM (XL30, Philips, Netherlands) and energy-dispersive-X-ray SEM (S-2500C, Hitachi, Japan), respectively. The SEM analyses were performed after mounting pieces of the sample on an aluminum stub and coating with platinum using a sputter coater (E1030, Hitachi, Tokyo, Japan). To confirm the change in acidity of the solution containing the nanocomposite, the pH of the solution containing the films was measured over time while shaking at 100 rpm in 37 °C.

**Mechanical Property Measurement.** The mechanical properties of the nanocomposites were instantiated through a universal testing machine (UTM; Instron 4464, Instron, USA). The analysis was carried out on the conditions with a gauge length of 5 cm and a crosshead speed of 1 cm/min according to ASTM D638-00. Finally, the mechanical properties of nanocomposites were analyzed with parameters such as tensile strength, elongation, tensile modulus, and the interfacial interaction parameters.

**In Vitro Cell Culture.** In this study, U-937 cells (a human hematopoietic cell line) and HUVECs were used, respectively. The U-937 cells were cultured in RPMI media containing 10% inactivated fetal bovine serum (FBS) and 1% penicillin/streptomycin at 37 °C in 5% CO<sub>2</sub> atmosphere. The HUVECs were cultured in EGM-2 media containing 5% inactivated FBS, 1% penicillin/streptomycin, heparin (5 U/mL), and human fibroblast growth factor (10 ng/mL) at 37 °C in 5% CO<sub>2</sub> atmosphere. All cell experiments were performed within 4–5 passages of cells.

**In Vitro Cell Viability Assays.** To determine the cell viability of U-937 cells and HUVECs, the Cell Counting Kit-8 (CCK-8, Dojindo Molecular Technology, Inc., Rockville, MD) assay was performed according to the manufacturer's protocol. The absorbance of the analytical reagent was measured at 450 nm through a microplate reader (Spectra Max M2, Molecular Device, USA).

**Measurement of Inflammatory Cytokine Levels.** Inflammatory cytokine levels were measured to investigate the inflammation induction of nanocomposites. Levels of TNF- $\alpha$  and IL-6 were measured by enzyme-linked immunosorbent assay (ELISA) in U-937 cells and HUVEC, respectively. To measure the level of TNF- $\alpha$ , U-937 cells were seeded in a 24-well plate and cultured in RPMI medium for 24 h. Then the cells were treated with the degradation product (1.0 mg) of nanocomposite for 24 h and the level of TNF- $\alpha$  in the culture medium was measured by ELISA (R&D systems, Minneapolis, MN). To measure the level of IL-6, HUVECs were seeded in 24-well plate and cultured in EGM-2 medium for 24 h. Then the cells were treated with the degradation product (1.0 mg) of nanocomposite for 24 h, and the level of IL-6 in the culture medium was measured by ELISA (R&D systems, Minneapolis, MN).

**In vivo tests.** Detailed experimental methods for *in vivo* animal experiments are described in the [Supporting Information](#).

## ASSOCIATED CONTENT

### Supporting Information

The Supporting Information is available free of charge on the ACS Publications website at DOI: [10.1021/acsnano.8b02365](https://doi.org/10.1021/acsnano.8b02365).

Experimental methods for *in vivo* tests; characterization of RA-Mg-OHs, RA-MG-OLAs nanoparticles, and PLGA/RA-Mg-OLAs composites; supporting results and discussion; histology and real-time PCR data for PLGA/RA-Mg-OLA scaffolds; information of antibodies used for IHC; information of primer sequences used for real-time PCR ([PDF](#))

## AUTHOR INFORMATION

### Corresponding Authors

\*E-mail: [dkhan@cha.ac.kr](mailto:dkhan@cha.ac.kr).

\*E-mail: [jhubbell@uchicago.edu](mailto:jhubbell@uchicago.edu).

### ORCID

Wooram Park: [0000-0002-4614-0530](https://orcid.org/0000-0002-4614-0530)

Youngjin Cho: [0000-0002-1435-6070](https://orcid.org/0000-0002-1435-6070)

Yoon Ki Joung: [0000-0001-8661-481X](https://orcid.org/0000-0001-8661-481X)

Dong June Ahn: [0000-0001-5205-9168](https://orcid.org/0000-0001-5205-9168)

Byung-Soo Kim: [0000-0001-5210-7430](https://orcid.org/0000-0001-5210-7430)

Jeffrey A. Hubbell: [0000-0003-0276-5456](https://orcid.org/0000-0003-0276-5456)

### Author Contributions

<sup>^</sup>E.L., C.H.K., and W.P. contributed equally.

### Notes

The authors declare no competing financial interest.

## ACKNOWLEDGMENTS

This work was supported by Basic Science Research Program (2017R1A2B3011121) and Bio & Medical Technology Development Programs (2014M3A9D3033887 and 2018M3A9E2024579) through the National Research Foundation of Korea funded by the Ministry of Science and ICT (MSIT), Republic of Korea.

## REFERENCES

- (1) Hollister, S. J. Porous Scaffold Design for Tissue Engineering. *Nat. Mater.* **2005**, *4*, 518.
- (2) Rezwani, K.; Chen, Q.; Blaker, J.; Boccaccini, A. R. Biodegradable and Bioactive Porous Polymer/Inorganic Composite Scaffolds for Bone Tissue Engineering. *Biomaterials* **2006**, *27*, 3413–3431.
- (3) Singh, L.; Kumar, V.; Ratner, B. D. Generation of Porous Microcellular 85/15 Poly(DL-lactide-co-glycolide) Foams for Biomedical Applications. *Biomaterials* **2004**, *25*, 2611–2617.
- (4) Kashte, S.; Jaiswal, A. K.; Kadam, S. Artificial Bone via Bone Tissue Engineering: Current Scenario and Challenges. *Tissue Eng. Regen. Med.* **2017**, *14*, 1–14.
- (5) Anderson, J. M. *In Vivo* Biocompatibility of Implantable Delivery Systems and Biomaterials. *Eur. J. Pharm. Biopharm.* **1994**, *40*, 1–8.
- (6) Anderson, J. M.; Rodriguez, A.; Chang, D. T. Foreign body reaction to biomaterials. *Seminars Immunology*; Elsevier, 2008; pp 86–100.
- (7) Danhier, F.; Ansorena, E.; Silva, J. M.; Coco, R.; Le Breton, A.; Préat, V. PLGA-based Nanoparticles: An Overview of Biomedical Applications. *J. Controlled Release* **2012**, *161*, 505–522.
- (8) Ellis, S. G.; Kereiakes, D. J.; Metzger, D. C.; Caputo, R. P.; Rizik, D. G.; Teirstein, P. S.; Litt, M. R.; Kini, A.; Kabour, A.; Marx, S. O. Everolimus-Eluting Bioresorbable Scaffolds for Coronary Artery Disease. *N. Engl. J. Med.* **2015**, *373*, 1905–1915.
- (9) Serruys, P. W.; Chevalier, B.; Sotomi, Y.; Cequier, A.; Carrié, D.; Piek, J. J.; Van Boven, A. J.; Dominici, M.; Dudek, D.; McClean, D. Comparison of an Everolimus-eluting Bioreabsorbable Scaffold with an Everolimus-Eluting Metallic Stent for the Treatment of Coronary Artery Stenosis (ABSORB II): A 3 year, Randomised, Controlled, Single-blind, Multicentre Clinical trial. *Lancet* **2016**, *388*, 2479–2491.
- (10) Iwasaki, Y.; Sawada, S.-i.; Ishihara, K.; Khang, G.; Lee, H. B. Reduction of Surface-induced Inflammatory Reaction on PLGA/MPC Polymer Blend. *Biomaterials* **2002**, *23*, 3897–3903.
- (11) Yoon, S. J.; Kim, S. H.; Ha, H. J.; Ko, Y. K.; So, J. W.; Kim, M. S.; Yang, Y. I.; Khang, G.; Rhee, J. M.; Lee, H. B. Reduction of Inflammatory Reaction of Poly(D, L-lactic-co-glycolic acid) Using Demineralized Bone Particles. *Tissue Eng., Part A* **2008**, *14*, 539–547.
- (12) Li, D.; Sun, H.; Jiang, L.; Zhang, K.; Liu, W.; Zhu, Y.; Fangteng, J.; Shi, C.; Zhao, L.; Sun, H. Enhanced Biocompatibility of PLGA Nanofibers with Gelatin/Nano-Hydroxyapatite Bone Biomimetics Incorporation. *ACS Appl. Mater. Interfaces* **2014**, *6*, 9402–9410.
- (13) Kum, C. H.; Cho, Y.; Joung, Y. K.; Choi, J.; Park, K.; Seo, S. H.; Park, Y. S.; Ahn, D. J.; Han, D. K. Biodegradable Poly(L-lactide) Composites by Oligolactide-grafted Magnesium Hydroxide for Mechanical Reinforcement and Reduced Inflammation. *J. Mater. Chem. B* **2013**, *1*, 2764–2772.
- (14) Anderson, J. M.; Shive, M. S. Biodegradation and Biocompatibility of PLA and PLGA Microspheres. *Adv. Drug Delivery Rev.* **1997**, *28*, 5–24.

- (15) Leenslag, J. W.; Pennings, A. J.; Bos, R. R.; Rozema, F. R.; Boering, G. Resorbable Materials of Poly(L-lactide): VII. *In Vivo* and *In Vitro* Degradation. *Biomaterials* **1987**, *8*, 311–314.
- (16) Matsusue, Y.; Yamamuro, T.; Oka, M.; Shikinami, Y.; Hyon, S. H.; Ikada, Y. *In Vitro* and *In Vivo* Studies on Bioabsorbable Ultra-high-strength Poly(L-lactide) Rods. *J. Biomed. Mater. Res.* **1992**, *26*, 1553–1567.
- (17) Suuronen, R.; Pohjonen, T.; Hietanen, J.; Lindqvist, C. A 5-year *In Vitro* and *In Vivo* Study of the Biodegradation of Polylactide Plates. *J. Oral Maxillofac. Surg.* **1998**, *56*, 604–614.
- (18) Park, T. G. Degradation of Poly(lactic-co-glycolic acid) Microspheres: Effect of Copolymer Composition. *Biomaterials* **1995**, *16*, 1123–1130.
- (19) Li, S.; Garreau, H.; Vert, M. Structure-property Relationships in the Case of the Degradation of Massive Poly( $\alpha$ -hydroxy acids) in Aqueous Media. *J. Mater. Sci.: Mater. Med.* **1990**, *1*, 198–206.
- (20) Hakkarainen, M.; Albertsson, A.-C.; Karlsson, S. Weight Losses and Molecular Weight Changes Correlated with the Evolution of Hydroxyacids in Simulated *In Vivo* Degradation of Homo- and Copolymers of PLA and PGA. *Polym. Degrad. Stab.* **1996**, *52*, 283–291.
- (21) Gresser, J. D.; Lewandowski, K.-U.; Trantolo, D. J.; Wise, D. L., Osteointegration and Dimensional Stability of Poly(D,L-lactide-co-glycolide) Implants Reinforced with Poly(propylene glycol-co-fumaric acid). In *Biomaterials Engineering and Devices: Human Applications*; Springer, 2000; pp 261–279.
- (22) Vhora, I.; Patil, S.; Patel, H.; Amrutiya, J.; Lalani, R.; Misra, A. Overview of Polyester Nanosystems for Nasal Administration. *Handbook of Polyester Drug Delivery Systems* **2016**, 291.
- (23) Giordano, G. G.; Chevez-Barrios, P.; Refojo, M. F.; Garcia, C. A. Biodegradation and Tissue Reaction to Intravitreal Biodegradable Poly(D, L-lactic-co-glycolic) Acid Microspheres. *Curr. Eye Res.* **1995**, *14*, 761–768.
- (24) Miller, R. A.; Brady, J. M.; Cutright, D. E. Degradation Rates of Oral Resorbable Implants (Polylactates and Polyglycolates): Rate Modification with Changes in PLA/PGA Copolymer Ratios. *J. Biomed. Mater. Res.* **1977**, *11*, 711–719.
- (25) Zhang, F.; Zhang, H.; Su, Z. Surface Treatment of Magnesium Hydroxide to Improve Its Dispersion in Organic Phase by the Ultrasonic Technique. *Appl. Surf. Sci.* **2007**, *253*, 7393–7397.
- (26) Lv, X.; Li, M.; Ma, X.; Ma, S.; Gao, Y.; Tang, L.; Zhao, J.; Guo, Y.; Zhao, X.; Wang, Z. In Situ Synthesis of Nanolamellas of Hydrophobic Magnesium Hydroxide. *Colloids Surf., A* **2007**, *296*, 97–103.
- (27) Yan, H.; Zhang, X.-h.; Wei, L.-q.; Liu, X.-g.; Xu, B.-s. Hydrophobic Magnesium Hydroxide Nanoparticles *via* Oleic Acid and Poly(methyl methacrylate)-Grafting Surface Modification. *Powder Technol.* **2009**, *193*, 125–129.
- (28) Vieira, C.; Evangelista, S.; Cirillo, R.; Lippi, A.; Maggi, C. A.; Manzini, S. Effect of Ricinoleic Acid in Acute and Subchronic Experimental Models of Inflammation. *Mediators Inflammation* **2000**, *9*, 223–228.
- (29) Kum, C. H.; Cho, Y.; Seo, S. H.; Joung, Y. K.; Ahn, D. J.; Han, D. K. A Poly(lactide) Stereocomplex Structure with Modified Magnesium Oxide and Its Effects in Enhancing the Mechanical Properties and Suppressing Inflammation. *Small* **2014**, *10*, 3783–3794.
- (30) Turcsanyi, B.; Pukanszky, B.; Tüdös, F. Composition Dependence of Tensile Yield Stress in Filled Polymers. *J. Mater. Sci. Lett.* **1988**, *7*, 160–162.
- (31) Zhu, G.; Mallery, S. R.; Schwendeman, S. P. Stabilization of Proteins Encapsulated in Injectable Poly(lactide-co-glycolide). *Nat. Biotechnol.* **2000**, *18*, 52.
- (32) Banas, A.; Teratani, T.; Yamamoto, Y.; Tokuhara, M.; Takeshita, F.; Osaki, M.; Kawamata, M.; Kato, T.; Okochi, H.; Ochiya, T. IFATS Collection: *In Vivo* Therapeutic Potential of Human Adipose Tissue Mesenchymal Stem Cells after Transplantation into Mice with Liver Injury. *Stem Cells* **2008**, *26*, 2705–2712.